The role of strigolactones in regulation of stomatal conductance and plant-pathogen interactions in *Arabidopsis thaliana*

Maria Kalliola[1], Liina Jakobson[2], Pär Davidsson[1], Ville Pennanen[1], Cezary Waszczak[3], Dmitry Yarmolinsky[2], Olena Zamora[2], E. Tapio Palva[1], Tarja Kariola[4], Hannes Kollist[3], Mikael Brosché[2,3]

Affiliations

[1]Viikki Plant Science Centre, Molecular and Integrative Biosciences Research Programme, Faculty of Biological and Environmental Sciences, University of Helsinki, Helsinki, Finland

[2]Institute of Technology, University of Tartu, Tartu, Estonia

[3]Viikki Plant Science Centre, Organismal and Evolutionary Biology Research Programme, Faculty of Biological and Environmental Sciences, University of Helsinki, Helsinki, Finland

[4]LUMA Centre Päijät-Häme, University of Helsinki, Lahti, Finland

Correspondence

Mikael Brosché, Viikki Plant Science Centre, Organismal and Evolutionary Biology Research Programme, Faculty of Biological and Environmental Sciences, University of Helsinki, Helsinki, Finland

Email: mikael.brosche@helsinki.fi

Abstract

The phytohormone strigolactone controls branching in *Arabidopsis thaliana*, but in recent years it has been shown to also affect many other plant functions. We previously showed that the strigolactone perception mutant *max2* has increased susceptibility to plant pathogenic bacteria as a result of increased stomatal conductance as well as alterations in hormonal signalling. Here we show that both strigolactone biosynthesis (*max3* and *max4*) and perception mutants (*max2* and *d14*) were significantly more sensitive to *Pseudomonas syringae* DC3000. Moreover, in response to *P. syringae* infection, high levels of SA accumulated in *max2* and this mutant was ozone sensitive. To search for the mechanisms that could explain pathogen and ozone sensitivity we performed gene expression experiments and several different assays that explore the function of guard cells and regulation of guard cell signalling.

Treatments with GR24 (a strigolactone analogue) resulted in very modest changes in defence related gene expression. In contrast, guard cell function was clearly impaired in *max2* and depending on the assay used, also in *max3*, *max4* and *d14*. Moreover, different stimuli (darkness, high CO_2 and ABA) that cause stomatal closure in wild-type plants were analysed in the strigolactone mutants. In darkness both strigolactone biosynthesis and perception mutants showed reduced stomatal closure, whereas the response to high CO_2 was impaired only in *max2* and *d14*. The response to ABA was not impaired in any of the mutants. To position the role of MAX2 in the guard cell signalling network, *max2* was crossed with mutants defective in ABA biosynthesis (*aba2*), in guard cell ABA signalling (*ost1*) and a scaffold protein required for proper ion channel activity (*ghr1*). The stomatal conductance of double mutants was consistently higher than the corresponding single mutants, suggesting that MAX2 acts in a signalling pathway that functions in parallel to the well characterized guard cell ABA signalling pathway. We propose that the impaired defence responses of *max2* is related to more open stomata that allows increased entry of bacteria or air pollutants like ozone. Furthermore, as MAX2 appears to act in a specific branch of guard cell signalling (related to CO_2 signalling), this protein could be one of the elusive components that allow guard cells to distinguish between different environmental conditions.

Introduction

Strigolactones are best known for their role in regulation of shoot branching in *Arabidopsis thaliana* by influencing polar auxin transport (Hayward et al 2009, Crawford et al 2010). However, in addition to shoot development, strigolactones affect several other processes such as senescence and responses to salinity and light stress (Shen et al 2007, Umehara et al 2008, Gomez-Roldan et al 2008). Moreover, recently Stes et al (2015) demonstrated that strigolactones contribute to tolerance to the leafy gall syndrome (caused by *Rhodococcus fascians*), which indicates their role in regulating plant-pathogen interactions. Strigolactones also affect drought tolerance by affecting stomatal conductance (Bu et al 2014, Ha et al 2014).

Strigolactones are synthesized mainly in roots and transported to shoots, however the route of transport is not clear (Kohlen et al 2011; Xie et al 2015). Both strigolactone synthesis and perception involve *MORE AXILLARY GROWTH (MAX)* proteins that act in a single pathway. MAX1, MAX3 and MAX4 catalyse strigolactone biosynthesis, while the perception require MAX2 and DWARF14 (D14) - the receptor of strigolactone (Al-Babili and Bouwmeester, 2015, Chevalier et al 2014, Waters et al 2012). MAX2 is an F-box protein that targets proteins for destruction as part of ubiquitin proteasome system (Lechner et al 2006, Stirnberg et al 2002). Strigolactones are proposed to be hydrolyzed by D14 resulting in a conformational change in the D14 protein, which facilitates interaction of D14 and SCF^{MAX2} (SKP1-CUL1-F-box), an E3 ligase functioning in ubiquitination (Lv et al 2017). Targets of MAX2 include SUPPRESSOR OF MORE AXILLARY GROWTH2-LIKE6 (SMXL6), SMXL7 and SMXL8 (Wang et al., 2015).

Stomata play a central role in carbon assimilation and stress responses as they regulate the uptake of CO_2 which is inevitably connected to the evaporative loss of water. Moreover, open stomata provide an entry point for air pollutants and plant pathogens (Vainonen and Kangasjärvi 2015, Melotto et al 2017). Guard cells which form the stomatal pore, respond to various endogenous and environmental stimuli by regulating their volume that in turn has a direct impact on the aperture of stomatal pores. Stomatal closure is induced by abscisic acid (ABA), pathogen-associated molecular patterns (PAMPs), high carbon dioxide (CO_2) concentration, darkness, drop in relative air humidity and air pollutants such as ozone (Melotto et al 2006, Merilo et al 2013). ABA biosynthesis starts from carotenoids and ABA2 (ABSCISIC ACID DEFICIENT2) catalyses the conversion of xanthoxin to abscisic aldehyde (González-Guzmán 2002). Analysis of the *aba2* mutant that express *ABA2* with either guard cell or phloem specific promoter show that both promoters could restore ABA levels and functional ABA responses, demonstrating effective transport of ABA between tissues (Merilo et al. 2018). ABA-induced stomatal closure is initiated after binding of the hormone by PYR/PYL/RCAR receptors leading to inactivation of PP2C phosphates and followed by release of SNF-related protein kinases (SnRK2s) such as OST1 (OPEN STOMATA1). OST1 together with Ca^{2+}-dependent protein kinases activate SLAC1 (SLOW ANION CHANNEL1) leading to stomatal closure (Merilo et al 2013). Another protein GUARD CELL HYDROGEN PEROXIDE-RESISTANT1 (GHR1) is required for stomatal closure and is proposed to act as a scaffold bringing together various proteins needed to initiate stomatal closure (Hua et al 2012, Sierla et al 2018).

We previously showed that the strigolactone perception mutant *max2* has increased susceptibility to plant pathogenic bacteria (*Pseudomonas syringae*) as a result from more open stomata and impaired stomatal closure in response to infection (Piisilä et al 2015). Further, we demonstrated that the *max2* mutant also exhibits other stress-related phenotypes such as decreased tolerance to apoplastic ROS, changes in stress-related gene expression, and hormonal signalling i.e. increased salicylic acid levels (Piisilä et al 2015). However, as MAX2 is known to participate in several signalling pathways and acts as a central regulator in both strigolactone and karrikin signalling (Li et al 2017), we set out to clarify the role of strigolactones in plant defence responses by analysis of strigolactone biosynthesis mutants (*max3, max4*) and their receptor (D14). Therefore, we analysed the role of the strigolactone pathway in pathogen sensitivity, defence to ROS and stomatal regulation using single and double mutants defective in various steps of strigolactone biosynthesis and perception. Furthermore, the possible interaction between ABA and strigolactone signalling was assessed with a new set of double mutants.

Materials and methods

Plant material

All mutants used in this study were in the Col-0 genetic background. The following mutants were obtained from the Nottingham Arabidopsis Stock Centre: *max2-1* (Stirnberg et al 2002), *max2-4* (SALK_028336), *max3-9* (Booker et al 2004), *max3-11* (SALK_023975), *max4-1* (Sorefan et al 2003) and *max4-7* (SALK_082552), *ost1-3* (*srk2e*, SALK_008068; Yoshida et al 2002), *aba2-11* (González-Guzmán et al 2002), *d14-1* (CS913109; Waters et al 2012), *sid2-2* (Wildermuth et al 2001). The *d14-seto5* and *max2-1 d14-seto5* (Chevalier et al 2014) were obtained from Pilar Cubas. The *ghr1-3* (GK_760C07; Sierla et al 2018) was donated by Jaakko Kangasjärvi. All mutants were genotyped by PCR based markers (Supplemental table 1).

The double mutants *aba2-11 max2-4*, *ghr1-3 max2-4* and *ost1-3 max2-4* were generated by crossing the respective single mutants with *max2-4* (pollen donor). Double homozygous plants were identified in F2 segregating progenies by PCR with gene-specific primers (Supplemental table 1).

Growth conditions

Growth conditions in University of Tartu (the gas-exchange experiments). Arabidopsis seeds were planted in a soil pot covered by a glass plate with a hole through which the plants were grown as described by Kollist et al (2007). The soil mixture contained 2:1 peat:vermiculite. Plants were grown in growth chambers in a 12 h photoperiod, 23°C/18°C temperature, 150 µmol m^{-2} s^{-1} light, and 70% relative humidity.

Growth conditions in University of Helsinki (all other experiments). Seeds were sown on a 1:1 peat:vermiculite mixture, vernalized in the dark for two days at 4°C, and germinated for one week. Next, plants were transferred to fresh pots to grow individually. Plants were grown in a growth room in 12 h light period (220 µmol m^{-2} s^{-1}), 23°C/18°C day/night temperature and 70 % relative humidity. One to two weeks before the experiment plants were moved into a growth chamber with similar temperature/light conditions.

For gene expression experiments with plants treated with GR24, seeds were surface sterilized with 70 % ethanol and 2 % Triton X-100, rinsed 3 times with 99 % ethanol and dried on a filter paper. Plants were grown *in vitro* on ½ MS plates for 2 weeks in 16 h light/8 h dark cycle (110 µmol m^{-2} s^{-1}), 23°C/18°C day/night temperature.

Pathogen assays

Pseudomonas syringae pv. *tomato* DC3000 were grown in King's B media at 28 °C overnight and the bacterial cells were collected by centrifugation at 6000 rpm for 8 min, and washed with 10 mM $MgCl_2$. The centrifugation was repeated, and the bacteria were suspended in 10 mM $MgCl_2$. OD_{600} was adjusted to 0.1, which equals to 10^7 cfu ml^{-1} of bacteria in spray medium. To reduce surface tension 0.02 % Silwet L-77 was added just before inoculation. 4-5 weeks-old plants were sprayed equally until their leaves were saturated with the spray medium. After inoculation plants were covered with plastic to maintain the humidity. The amount of bacterial cells was determined at 1.5 h and 48 h post inoculation. For each biological replicate, three leaf discs from three separate leaves were analysed. Leaf discs were surface sterilized with 70 % ethanol, washed with MQ water and ground in 0.2 ml of 10 mM $MgCl_2$, after which the volume was adjusted to 1 ml. From the dilution series the aliquots of different dilutions were pipetted to King's B media plates and grown for 2 days at 28 °C.

Measurement of free SA levels

Free salicylic acid was measured using a modified biosensor-based method based on a protocol described by DeFraia et al 2008. The bacterial biosensor strain *Acinetobacter* sp. ADPWH_*lux* (Huang et al 2005, Huang et al 2006) was grown overnight in LB medium at 37°C, after which the culture was diluted 1:20 and grown to an OD_{600} of 0.4. Leaf samples of 30 day-old plants were collected 27 h post spray inoculation with *Pst* DC3000 (OD_{600} = 0.2). A leaf disc (9 mm diameter) was cut from the 5th, 6th and 7th leaf of each plant and the three discs were homogenized in 200 µl of LB-medium. To count bacterial cfu, we took 8 µl aliquot, and the rest of sample was centrifuged for 15 min 21000 g. 20 µl of the supernatant was mixed with 30 µl of LB-medium and 50 µl of 1:100 diluted biosensor culture (OD600 = 0.004) on a white 96-well plate. The plate was incubated

at 37 °C for one hour without shaking, after which the luminescence was measured with Perkin Elmer EnSpire 2300 plate reader. For standard curve, 0, 5, 10, 15 and 20 ng of sodium salicylate in 30 µl of LB-medium were mixed with 20 µl of plant extract from *sid2-2* plants and 50 µl of the diluted biosensor strain. The standard curve was measured parallel with the samples. Due to non-linearity of the standard curve values, separate linear best-fit lines were fitted for low (0-10 ng) and high (10-20 ng) amounts of salicylic acid standard as described by (DeFraia et al 2008). The luminescence values of the samples were converted to estimated masses of salicylic acid based on the standard curves and reported as ng cm^{-2}. Statistical analysis were performed R programming environment and figures were prepared R with ggplot2 package (R Core Team 2018, Wickham 2016).

Ozone exposure and ion leakage analysis

The ozone exposure was conducted with 350 nL L^{-1} of ozone gas for 6 hours on 4-5 week old plants as described by Overmyer et al 2000. The relative ion leakage was measured as conductivity in 0, 6 and 24 hours after beginning of ozone exposure. The whole rosette was cut and put to milli-Q water. There were 4 biological repeats for each time point from each plant line. The conductivity was measured using Horiba Twin Cond Conductivity Meter B-173.

Expression analysis by qPCR

Pseudomonas syringae pv. *tomato* DC3000 bacteria was grown and infection was done with OD = 0.1 on 4-5 week old plants. The samples were taken 0 (i.e. non-infected), 3, 6, 24 and 48 h after the infection.

GR24 (from Chiralix) was dissolved in DMSO and a solution of 10 µM GR24 and 0,01 % of Silwet L-77 was poured into the wells of a 6-well multi plate. The control solution consisted of the corresponding amounts of DMSO and Silwet. Whole intact 14 day-old in vitro grown Col-0 seedlings were put into the wells and samples were collected after 3 hours.

RNA was isolated with GeneJET Plant RNA Purification Mini Kit (Thermo Scientific). RNA (3 µg in GR24 assay/2 µg in Pseudomonas infection) was DNAseI treated and reverse transcribed with Maxima RT and Ribolock Rnase inhibitor (Thermo Scientific, formerly Fermentas) according to the manufacturer instructions. After cDNA synthesis the reactions were diluted to a final volume of 100 µl. qPCR was performed in triplicate using 5x HOT FIREPol EvaGreen qPCR Mix Plus (Solis Biodyne). The cycle conditions with Bio-Rad CFX384 were: 1 cycle initiating with 95°C 10 min, 50 cycles with 95°C 15s, 60°C 30s, 72°C 30s and ending with melting curve analysis. Normalization of the data was performed in qBase 3.0 (Biogazelle), with the reference genes PP2AA3, TIP41 and YLS8 in GR24 assay/ F-box protein AT5G15710 in Pseudomonas infection. Primer amplification efficiencies were determined in qBase from a cDNA dilution series. All primers are listed in supplemental table 1.

Stomatal conductance

The porometer measurements were done on 5-6 week old plants with an AP4 porometer (Delta-T Devices, Cambridge, UK). The plants were measured according to the phenotype-based growth stage (Boyes et al 2001) and 2-3 leaves per each growth stage was measured from each plant and altogether minimum 20 plants were measured from each plant line. The age of the plants was 5-6 weeks when the rosettes reached their maximal size but the flower buds were not yet visible.

The basal level of whole-plant stomatal conductance and stomatal responses to CO_2, darkness and 5 µM ABA foliar spray were measured with a custom-made gas exchange measurement device in University of Tartu described in details by Kollist et al 2007. The unit of stomatal conductance mmol m^{-2} s^{-1} reflects the amount of H_2O moles that exits the plant through stomata per m^2 of leaf area per second. The age of the plants was 3-4 weeks when they were measured. Due to the bushy phenotype of several studied mutants, the rosette area of all plants was calculated by separating the leaves and measuring individually. Prior to the experiment,

plants were acclimated in the measurement cuvettes in ambient CO_2 concentration (~400 ppm), 100 µmol m^{-2} s^{-1} light, and ambient humidity (RH 65%–80%) for at least 1 h or until stomatal conductance was stable.

ABA-induced stomatal closure was induced by foliar spray of 5 µM ABA solution (5 µM ABA, 0.012% Silwet L-77, and 0.05% ethanol). At time point T=0 min, plants were removed from the measuring cuvettes and sprayed with either 5 µM ABA solution or control solution (0.012% Silwet L-77 and 0.05% ethanol). Thereafter, plants were returned to the cuvettes and stomatal conductance was monitored for 40 min.

Foliar spray with GR24 was conducted as following: at time point T=0 min preincubated plants were removed from the measuring cuvette and 10 µM GR24 solution (10 µM GR24 (Chiralix, The Netherlands), DMSO, 0.012% Silwet L-77) was applied with a spray bottle 5 times approx. 30 cm from the rosette so that the plant would look slightly wet. The plants were returned to the measuring cuvettes to dry and starting from T=8 min the plants were monitored for 56 minutes.

Statistical analyses of gas exchange data were performed with Statistica, version 7.1 (StatSoft Inc., Tulsa, Oklahoma, United States). All effects were considered significant at $p < 0.05$.

Accession numbers

ABA2 - AT1G52340, MAX2 – AT2G42620, OST1 - AT4G33950, GHR1 - AT4G20940, MAX3 - AT2G44990, MAX4 - AT4G32810, D14 - AT3G03990, ICS1/SID2 - AT1G74710 , PR1 - AT2G14610, FRK1 - AT2G19190, NCED3 - AT3G14440, GRX480 - AT1G28480, AXR3/IAA17 - AT1G04250, PP2AA3 - AT1G13320, YLS8 - AT5G08290, TIP41- AT4G34270.

Supporting Information

Supporting Information Figure 1. The sensitivity to pathogens in darkness.

Supporting Information Figure 2. Growth of *P. syringae* in free SA analysis.

Supporting Information Figure 3. The time course data used to calculate the bar graphs of Figure 7(c)–7(h).

Supporting Information Figure 4. The phenotypes of the Arabidopsis Col-0 and the mutant plants involved in the experiments.

Supporting Information Table 1. The PCR primers used in genotyping and qPCR primers used in gene expression analysis.

Results

Strigolactone affects sensitivity to pathogens in Arabidopsis

Plant defence against pathogens use a network of interacting signalling pathways where several plant hormones are key components (Overmyer et al 2018). Recently, strigolactones were identified as an additional component that regulates drought and pathogen responses (Bu et al 2014, Ha et al 2014, Piisilä et al 2015). Here, we further explored the mechanism of strigolactones in sensitivity to pathogens by analysis of strigolactone receptor (D14) mutants and strigolactone synthesis (MAX3 and MAX4) mutants in order to find biological processes regulated by strigolactones.

Spray infection with *P. syringae* DC3000 allows quantification of pathogen sensitivity in relation to stomatal immunity, as the bacteria need to enter the plant through stomata to multiply (Melotto et al 2006). Interestingly, *max2* mutants exhibited increased sensitivity to *P. syringae* DC3000 infection (Figure 1; OD_{600} = 0.1) compared to Col-0 already early in the infection, 1.5 hours post inoculum (hpi). Strigolactone sensing (*max2*), the receptor (*d14*) and synthesis (*max3* and *4*) mutants were all more sensitive to *P. syringae* DC3000 infection at 48 hpi (Figure 1). Moreover, at 48 hpi some differences were observed between the mutants, notably the *max2-4* allele (a SALK T-DNA line) had a stronger phenotype than *max2-1* (an ems mutant; Stirnberg et al 2002). Similarly, the Wisconsin tDNA knock-out line *d14-1* had a stronger phenotype than *d14-*

seto5 (an ems mutant; Chevalier et al 2014). In order to assess the role of stomatal openness in the infection, a similar infection was also done in an inverted light rhythm i.e. the plants were infected in darkness when the stomata are normally closed but the result was rather similar to infection in normal light conditions (Suppl. data 1). We conclude that both strigolactone biosynthesis and perception mutants were all significantly more sensitive to *P. syringae* DC3000 spray infection than Col-0 at 48 hpi.

max2 accumulate high level of free salicylic acid in response to *P. syringae* DC3000

The plant hormone salicylic acid (SA) has a key role in defence against pathogen infection (Fu and Dong 2013, Pieterse 2012). We measured free SA levels in Col-0 and the strigolactone mutants at 27 hpi after spray infection with *P. syringae* DC3000 (Figure 2; OD_{600} = 0.2, which was a higher inoculum than used in Figure 1; OD_{600} = 0.1). Simultaneously, we measured the extent of pathogen growth at the same time point (Supporting Information Figure 2). We included the SA biosynthesis mutant *sid2,* which does not accumulate SA in response to pathogens (Wildermuth et al 2001), as a control for the assay. High levels of SA accumulated in both *max2* alleles (Figure 2), consistent with our previous measurements of SA after pathogen infection (Piisilä et al 2015). In contrast, the levels of SA did not increase to significantly higher levels in either strigolactone biosynthesis mutants or the receptor (*d14*). At this higher pathogen inoculation and also earlier (27 hpi vs 48 hpi) time point, only the *max2* mutants were significantly more sensitive (Supporting Information Figure 2). We conclude that the *max2* mutant is pathogen sensitive also when a higher inoculum of bacteria is used at an earlier time point, but the differences in sensitivity of strigolactone biosynthesis and perception mutants were only clear with smaller bacterial inoculum at a later time point.

Strigolactone is not a major regulator of defence gene expression

The role of strigolactones in Arabidopsis is best described in branching (Gomez-Roldan et al 2008, Goulet and Klee 2010, Crawford et al 2010, Waldie et al 2014). Microarray analysis to find strigolactone regulated genes was previously performed with GR24 (a strigolactone analog) (Mashiguchi et al 2009). 64 genes had significantly altered expression and the magnitude of altered gene expression (i.e. fold change) in the GR24 regulated genes was small (Mashiguchi et al 2009). To test if GR24 can regulate genes related to pathogen defense, we treated 10 days old in vitro grown Col-0 with 10 µM GR24 for 3 hr and measured gene expression with real-time quantitative PCR (qPCR). Expression of the well-known pathogen-responsive genes *PR1* (*PATHOGENESIS-RELATED GENE 1*, a late response gene indicating activated SA response, Uknes et al 1992) and *FRK1* (*FLG22-INDUCED RECEPTOR-LIKE KINASE 1*, an early flg22 response marker gene, Asai 2002) decreased, although this was not statistically significant. Consistent with a role for strigolactone together with auxin in regulation of plant development, expression of *AXR3/IAA17 (AUXIN RESISTANT 3/ INDOLE-3-ACETIC ACID INDUCIBLE 17)* increased (Figure 3). Expression of *GRX480* (a glutaredoxin that regulates protein redox state) also increased. *GRX480* expression is regulated by several pathways including SA and ROS (Blanco et al 2009, Koornneef and Pieterse 2008, Pieterse et al 2012, Xu et al 2015a).

We also monitored the expression of *PR1*, *FRK1* and *NCED3* (*NINE-CIS-EPOXYCAROTENOID DIOXYGENASE 3,* a gene encoding a protein that is catalysing a major step in ABA biosynthesis (Fan et al 2009, Tan et al 2003, Wang et al 2011) in *P. syringae* infected *max2* and *d14* plants. A few subtle differences were observed including increased expression of PR-1 at an early time point (3 hr) in *max2-1* and increased expression of *NCED3* at the start (0 hr) and end (48 hr) of the experiment (Figure 3). As a relatively large variation was observed between different biological repeats, it is possible that some subtle differences between mutants might be obscured, but overall it appears that strigolactone perception and signalling is not a major regulator of defence related genes.

Strigolactone perception mutants, but not biosynthesis mutants were ozone sensitive

Treatment of plants with ozone is a method to explore plant sensitivity to oxidative stress. Ozone enters plants via stomata and immediately degrades to ROS ($O_2^{\bullet-}$ and H_2O_2) in the apolastic space of plant cells, which initiates cell death signalling and leads to visible dead tissue lesions in plants (Overmyer et al 2018, Vahisalu et al 2010, Vainonen and Kangasjärvi 2015). Importantly, as ozone enters the plant through stomata, the mechanisms of plant sensitivity to this air pollutant can broadly be divided into stomata dependent or independent mechanisms (Xu et al 2015b, Vainonen and Kangasjärvi, 2015). We assessed the extent of ozone damage using ion leakage after a 350 nL L^{-1} treatment for 6 hours and measured ion leakage before ozone exposure (0h) and in two time points (6 h and 24 h) after beginning of ozone exposure (Figure 4). Similar to the high inoculation with *P. syringae* (Supporting Information Figure 2), only the *max2* mutants were ozone sensitive. As also seen in the pathogen infection, the *max2-4* allele had a stronger phenotype than *max2-1*. The ion leakage 24 hours after beginning of exposure was also higher in *max2-1 14-seto5* double mutant plants than in *max2-1* or *d14-seto5* plants. The differential response of *max2* versus the biosynthesis and perception mutant suggest that MAX2 might act in additional signalling pathways beyond strigolactone signalling.

Strigolactone does not directly regulate the stomatal aperture.

Strigolactone perception and biosynthesis mutants were more *Pseudomonas* sensitive (Figure 1). However, changes in SA accumulation or gene expression could not explain this sensitivity. As spray infection require the bacteria to enter through stomata, signalling in guard cells leading to closure may be one of the primary functions of strigolactones. To explore this possibility we used various stomatal assays and mutants to further study strigolactone regulation of guard cell function (Figures 5 – 8). We tested the ability of GR24 to induce quick stomatal responses within an hour after application on the leaves in a system with intact plants (Kollist et al 2007, Merilo et al 2015). For this we sprayed the Col-0 rosettes with 10 µM GR24 solution and followed the stomatal conductance thereafter. No change in stomatal conductance after the foliar spray was detected neither with mock nor with GR24 (Figure 5a).

We also tested the ability of GR24 to close stomata at a longer time frame. GR24 is not soluble in water and in the literature different methods have been used to dissolve this chemical. We prepared a stock of GR24 in DMSO or acetone and diluted to 5 µM in water with 0.02 % Silwet L-77 and sprayed on Col-0 plants. Stomatal apertures was measured 24 hours after spraying using the protocol by Chitrakar and Melotto (2010). This late timepoint was selected to find out about the possible slower long-term effects on stomatal openness. No significant effect by GR24 on stomatal aperture was observed (Figure 5b).

Stomatal conductance measured with a porometer is higher in strigolactone-related mutants of different developmental stages

Various types of methods are available to measure stomatal conductance and thus get an estimate for how open the stomata are. We first measured stomatal conductance with a porometer, in which the sensor head is clipped onto a single leaf and the conductance is measured from only the lower i.e. abaxial side of the leaf. We used 5-6 weeks-old plants and measured leaves at different developmental stages 1-2, 3-4 and 5 (Boyes et al 2001, which roughly corresponds to old, middle age and young leaves). Both strigolactone perception and biosynthesis mutants had higher stomatal conductance at all leaf developmental stages (Figure 6). Notably, the *max2-4* allele had significantly higher conductance than the *max2-1* allele at older leaf age (Figure 6).

Stomatal conductance in intact plants and in response to darkness, high CO_2 and ABA.

Porometer measurements require touching of the plant and clipping the sensor head onto the leaf, which could for example activate touch related signalling. To measure the stomatal conductance of intact whole

plant rosettes we used a multi-cuvette gas exchange system (Kollist et al 2007), in which the plant is inserted into the machine without any touching. The system also allows a change of stimuli including darkness and increased CO_2. In contrast to the porometer measurements (Figure 6), only the *max2* alleles (and *max2-1 d14-seto5*) displayed increased stomatal conductance (Figures 7a and 7b).

Next we measured the response of the mutants to several other stimuli: darkness, high CO_2 and ABA (Figure 7 that are causing a stomatal closure in wild-type plants (Assmann and Jegla 2016, Merilo et al 2013). In darkness both strigolactone biosynthesis (*max3*, *max4*) and perception (*max2*, *d14*) mutants had significantly slower rate of stomatal closure. High CO_2 leads to stomatal closure and this response was impaired in *max2* and *d14* (Figures 7E and 7F). The stomatal response to ABA was not impaired, and instead an enhanced stomatal closure rate was observed in *max2-1*, possibly due to more open stomata of *max2-1* before ABA treatment (Figures 7G and 7H).

Most of our knowledge on regulation of guard cell signalling is in the context of ABA signalling (Merilo et al 2018); and very few regulators specific for other stimuli have been found (Engineer et al 2016). Thus the differential response of especially *max2* with a defective response towards high CO_2 and darkness and normal to enhanced response towards ABA, adds a new regulatory layer in guard cell signalling. As an F-Box protein, MAX2 might be involved in the targeted degradation of some other regulatory component in guard cell signalling.

MAX2 regulates stomatal function independent of ABA signalling

Of the different mutants we used to study the role of strigolactones, the *max2* mutant appeared special as it was the only mutant with ozone sensitivity and consistently higher stomatal conductance (Figures 4 and 7). To further explore the function of MAX2 in the guard cell signalling network, we crossed *max2* with mutants defective in ABA biosynthesis (*aba2*), in guard cell ABA signalling (*ost1*) and a scaffold protein GHR1 (*ghr1*) that is required for activation of the guard cell anion channel SLAC1. The double mutants all had significantly higher stomatal conductance than the corresponding single mutants (Figure 8), suggesting that MAX2 acts in a signal pathway that functions in parallel to the well characterized stomatal ABA signalling pathway.

Discussion

Plant defence responses to pathogen infection are highly complex and include many different signalling pathways (Koornneef and Pieterse 2008, Pieterse et al 2012). While hormones associated with stress e.g. salicylic acid, jasmonic acid, ethylene and abscisic acid have long been studied for their role in pathogen responses, also hormones typically associated with development influence the outcome of plant-pathogen interactions (Pieterse et al 2009). While the function of strigolactones in Arabidopsis was initially characterized for their role in branching (Bennett et al 2006, Hayward 2009, Stirnberg et al 2007), they appear to be important in pathogen sensitivity. Both mutants involved in strigolactone sensing (*max2*, *d14*) and biosynthesis (*max3* and *4*) were more sensitive to *P. syringae DC3000* spray infection than Col-0. However, given the differential response when higher inoculation was applied, where only *max2* showed increased sensitivity (Supporting Information Figure 2), it seems like the role of strigolactone is better described as a modulator of the defence response rather than a master regulator. Similarly the very modest response of defence genes to the application of the synthetic strigolactone analog GR24 (Figure 3 and Mashiguchi et al 2009), also indicates that strigolactones are not direct regulators of defence signalling.

We propose that the role of strigolactones and especially MAX2 in plant defence, is related to the regulation of stomatal function, which subsequently influence defence responses. This was clearly indicated by increased plant ozone sensitivity in *max2* mutant plants (Figure 4). Arabidopsis mutants and accessions with more open stomata are ozone sensitive as more ozone can enter the plant (Overmyer et al 2008, Brosché et al 2010). Similarly more open stomata would also allow higher entry of some bacteria like *P. syringae*. Additionally, the impaired stomatal closure in response to *P. syringae* infection likely contributes to sensitivity (Piisilä et al 2015). The strong *max2-4* allele was clearly more impaired than the weak *max2-1* allele as seen in pathogen susceptibility and ozone sensitivity. When weak alleles of *max2* (*max2-1*) and *d14* (*d14-seto5*) were combined in the double *max2-1 d14seto5* a similar phenotype to the strong *max2-4* was observed in pathogen (48 hpi) and ozone (24 h) responses (Figures 1and 3). This is consistent with the current understanding of D14 and MAX2 interacting in strigolactone perception (Lv et al 2017). However, as *d14-1* and biosynthesis mutants *max3* and *max4* were not ozone sensitive, this suggest that MAX2 has a more versatile role in stress responses than the other strigolactone related proteins. Previously MAX2 was also shown to have a role in karrikin signalling (Li et al 2017), pointing towards different signalling roles for this F-box protein, possibly by targeting the degradation of proteins in different signalling pathways.

To further evaluate the role of strigolactones in regulation of guard cell signalling we used several different methods and genetic tools. To our surprise we could not observe GR24 induced stomatal closure in either stomatal aperture or stomatal conductance assays (Figure 5). Ha et al (2014) rescued the drought phenotype of the strigolactone biosynthesis (*max3* and *max4*) mutants with strigolactone spray. Moreover, Lv et al (2017) showed by using epidermal peels that the stomata close in response to GR24 and strigolactones were concluded to be common regulators of stomatal closure *in planta* (Zhang et al 2018). One challenge in using GR24 is that no standard method for dissolving this chemical is established and possibly the solvent of GR24 might affect the results. Thus, we tried to dissolve GR24 both in DMSO and acetone but neither of them resulted in clear differences from mock in the size of stomatal aperture or in stomatal conductance.

There are several methods to measure stomatal function and first we performed a classical porometer measurement in order to explore if the growth stage (or age) of the leaves affected stomatal conductance. All of the strigolactone biosynthesis and perception mutants had a higher stomatal conductance except for *d14-seto5* (Figure 6) that consistently had a weaker phenotype than the other mutants, which can be seen also in the growth phenotype (Supporting Information Figure 3). As the strigolactone mutants have a “bushy” phenotype (Supporting Information Figure 3), and often leaves that lie on top of each other, the porometer measurements has the advantage that it measures a specific area independent from the rest of the plant. However, the data provided by the porometer is also limited, since the porometer sensor area is rather small and thus only a small area of a leaf is measured and we only measured the abaxial side of the leaf.

To complement the porometer data we used a system that measures the stomatal conductance of the whole rosette using a customized gas-exchange device which allows measurement of intact plants and responses

to stomata-affecting factors, such as CO_2 concentration, darkness and the phytohormone ABA in real-time (Kollist et al 2007). Here it becomes critical to have an accurate measurement of total leaf area, as this is one of the parameters used to get the stomatal conductance values. In contrast to porometer measurements, only *max2* and *max2 d14* mutants had more open stomata when the intact whole rosettes were measured (Figures 7a and 7b.). The difference between this result and the porometer results might have several explanations: (1) in promoter measurements only a limited area of a leaf can be measured and also handling the plants in the porometer measurements requires touching the leaves. (2) In intact plants the "bushy" phenotype with overlapping leaves of the strigolactone mutants might create a microclimate that alters stomatal conductance. (3) As porometer measurements were performed in Helsinki and stomatal conductance in intact plants in Tartu some other factor in growth conditions could sensitize the biosynthesis mutants (*max3*, *max4*) to have more open stomata in the Helsinki growth conditions. Further research might resolve this issue, but given the consistent phenotype of *max2* across several different assays and growth conditions, the response of this mutant strongly suggests an important role for MAX2 in guard cell signalling.

Testing stomatal responses to several different treatments showed that high CO_2-induced stomatal closure was impaired in *max2* and *d14-1* (Figures 7e and 7f). A sudden darkness treatment during the normal light period is partially initiated by the same mechanism as CO_2 signaling. Removal of light will stop photosynthesis and this leads to increase of CO_2 concentration inside the leaf, similar to the situation when elevated CO_2 is applied. The darkness-induced stomatal closure was reduced in *max2, max3, max4* and *d14-1*; i.e the response to darkness was more broadly impaired than the response to high CO_2. Of the different stimuli and treatments that lead to stomatal closure, the response to darkness might be the least studied. Thus, the impaired darkness response in both strigolactone biosynthesis and perception mutants opens the possibility for further studies into this branch of guard cell signaling.

To further study the relationship between strigolactone and ABA, we examined if ABA signalling and *MAX2* share the same elements in guard cell signalling and crossed *max2* with other guard cell signalling mutants *ost1*, *ghr1* and the ABA biosynthesis mutant *aba2.* The resulting double mutants (*max2 ghr1*, *max2 ost1* and *max2 aba2*) had a higher stomatal conductance than any of these mutants individually. Thus, it appears that MAX2 functions on a parallel pathway to ABA signalling (see also Lv et al 2017). As very few regulators of ABA independent guard cell signalling have been found (Assman and Jegla 2016, Engineer et al 2016), the impaired CO_2 and darkness response in *max2* implicate that the F-Box protein MAX2 has a crucial role in targeting some important guard cell regulator to ubiquitin mediated protein degradation. This regulator would not be any of the well-known components of the ABA signalling pathway, e.g. the PYR/PYL receptors, PP2C phosphatases or OST1 kinase (Assman and Jegla 2016, Engineer et al 2016). A future screen for MAX2 interacting proteins using e.g. MAX2 co-immunoprecipitation from isolated guard cells could be used to unravel other components of this specific branch of guard cell signalling and give new information on how different signalling pathways interact to regulate stomatal function.

Acknowledgement

This study was financially supported by the Academy of Finland Center of Excellence in Molecular Biology of Primary Producers 2014-2019 (grant 307335). C.W. is funded by the Academy of Finland (decision #294580). Moreover, we would like to thank support from Doctoral Program of Integrative Life Science (ILS) and Doctoral Program in Plant Sciences (DPPS). We thank Leena Grönholm for technical assistance in plant growth facilities. We would also like to thank Aapo Kalliola for providing a program for automatic leaf area calculation and Pilvi Ackté for technical assistance.

Supplemental Data

Supporting Information Figure 1. The sensitivity to pathogens in darkness is affected both in strigolactone sensing (*max2*), the receptor (*d14*) and synthesis (*max3* and *4*) mutants. The spray infection with *P. syringae* DC3000 was performed during the dark period of 12 h light rhythm 6 hours after the darkness was applied. In 48 hours post inoculation the infection is in general weaker than when performed in normal light rhythm but otherwise the light-rhythm dependent differences are small.

Supporting Information Figure 2. Growth of *Pseudomonas syringae* DC3000 in the same samples used in salicylic acid assay (Figure 2). Bacterial growth was quantified 27 hours after spray infection (OD600 = 0.2) in wild-type (Col-0), strigolactone signaling (*max2-1*, *max2-4*, *d14-1* and *d14-seto5*) and biosynthesis mutants (*max3* and *max4*). Salicylic acid biosynthesis mutant (*sid2-2*) was included as a control for no accumulation of free salicylic acid salicylic acid assay. Each dot represents one plant. In total, seven to eight plants were used per line. The experiment were performed three times with similar results. Box plots are summarising data by showing the median, and first and third quartiles. Whiskers are extending to a maximum of 1.5 × interquartile range beyond the box. Different letters indicate significant differences ($P < 0.05$) as determined by Kruskal-Wallis Rank Sum test followed by Pairwise Wilcoxon Rank Sum tests with multiple testing correction to p-values using Holm method.

Supporting Information Figure 3. The time course data of stomatal conductance used to calculate the bar graphs of Figure 7(c)–7(h).

Supporting Information Figure 4. The phenotypes of Arabidopsis Col-0 and the mutant plants involved in the experiments. The phenotype of 4-5 weeks-old plants. The size of the growth pot for all the plants is 7x7 cm.

Supporting Information Table 1. The PCR primers used in genotyping and qPCR primers used in gene expression analysis.

References

Al-Babili S., Bouwmeester H.J. 2015. Strigolactones, a novel carotenoid-derived plant hormone. Annu Rev Plant Biol. 66:161-86.

Asai T., Tena G., Plotnikova J., Willmann M.R., Chiu W.L., Gomez L., Boller T., Ausubel F.M., Sheen J. 2002. MAP kinase signalling cascade in *Arabidopsis* innate immunity. Nature, 415; 6875: 977-983.

Assmann S.M., Jegla T. 2016. Guard cell sensory systems: recent insights on stomatal responses to light, abscisic acid, and CO2. Current Opinion in Plant Biology. 33. 10.1016/j.pbi.2016.07.003.

Bennett T., Sieberer T., Willett B., Booker, J., Luschnig, C., Leyser, O. 2006. The Arabidopsis MAX pathway controls shoot branching by regulating auxin transport. Curr. Biol. 16: 553–563.

Blanco F., Salinas P., Cecchini N. M., Jordana X., Van Hummelen P., Alvarez M. E., Holuigue L. 2009. Early genomic responses to salicylic acid in *Arabidopsis*. *Plant Mol. Biol.* 70, 79–102.

Booker J., Auldridge M., Wills S., McCarty D., Klee H., Leyser O. 2004. MAX3/CCD7 is a carotenoid cleavage dioxygenase required for the synthesis of a novel plant signalling molecule. Curr Biol 14: 1232–1238.

Boyes D.C., Zayed A.M., Ascenzi R., McCaskill A.J., Hoffman N.E., Davis K.R., Görlach J. 2001. Growth stage-based phenotypic analysis of Arabidopsis: a model for high throughput functional genomics in plants. Plant Cell. 13: 1499-1510.

Brosché M., Merilo E., Mayer F., Pechter P., Puzõrjova I., Brader G., Kangasjärvi, J., Kollist, H. 2010. Natural variation in ozone sensitivity among Arabidopsis thaliana accessions and its relation to stomatal conductance. Plant Cell Environ. 33, 914–925.

Bu Q., Lv T., Shen H., Luong P., Wang J., Wang Z., Huang Z., Xiao L., Engineer C., Kim T.H., Schroeder J.I., Huq E. 2014. Regulation of drought tolerance by the F-box protein MAX2 in Arabidopsis. Plant Phys. 164:424–39.

Chevalier F., Nieminen K., Sánchez-Ferrero J.C., Rodríguez M.L., Chagoyen M., Hardtke C.S., Cubas P. 2014. Strigolactone promotes degradation of DWARF14, an α/β hydrolase essential for strigolactone signaling in Arabidopsis. Plant Cell 26: 1134–1150.

Chitrakar R., Melotto M. Assessing stomatal response to live bacterial cells using whole leaf imaging. 2010. J. Vis. Exp. 44:2185.

Crawford S., Shinohara N., Sieberer T., Williamson L., George G., Hepworth J., Müller D., Domagalska M.A., Leyser O. 2010. Strigolactones enhance competition between shoot branches by dampening auxin transport. Development 137: 2905–2913.

DeFraia C.T., Schmelz E.A., Mou Z. 2008. A rapid biosensor-based method for quantification of free and glucose-conjugated salicylic acid. Plant Methods 4:28.

Engineer C.B., Hashimoto-Sugimoto M., Negi J., Israelsson-Nordström M., Azoulay-Shemer T., Rappel W.-J., Iba K., Schroeder J.I. 2016. CO2 sensing and CO2 regulation of stomatal conductance: advances and open questions. Trends Plant Sci. 21; 16–30.

Fan J., Hill L., Crooks C., Doerner P., Lamb C. 2009. Abscisic acid has a key role in modulating diverse plant-pathogen interactions. Plant Physiol. 150:1750–61.

Fu Z. Q., Dong X. 2013. Systemic acquired resistance: Turning local infection into global defense. Annu. Rev. Plant Biol. 64, 839–863.

Gomez-Roldan V., Fermas S., Brewer P.B., Puech-Pages V., Dun E.A., Pillot J.P., Letisse F., Matusova R., Danoun S., Portais J.C., Bouwmeester H., Bécard G., Beveridge C.A., Rameau C., Rochange S.F. 2008. Strigolactone inhibition of shoot branching. Nature: 455:189–194.

González-Guzmán M., Apostolova N., Belles J.M., Barrero J.M., Piqueras P., Ponce M.R., Micol J.L., Serrano R., Rodríguez P.L. 2002. The short-chain alcohol dehydrogenase ABA2 catalyzes the conversion of xanthoxin into abscisic aldehyde. Plant Cell 14, 1833–1846.

Goulet C., Klee H.J. 2010. Climbing the branches of the strigolactones pathway one discovery at a time. Plant Physiology; 154:493-496.

Ha C.V., Leyva-González M.A., Osakabe Y., Tran U.T., Nishiyama R., Watanabe Y., Tanaka M., Seki M., Yamaguch, S., Dong N.V., Yamaguchi-Shinozaki K., Shinozaki K., Herrera-Estrella L., Tran, L.-S. P. 2014. Positive regulatory role of strigolactone in plant responses to drought and salt stress. Proc. Natl. Acad. Sci. USA. 111, 851–856.

Hayward A., Stirnberg P., Beveridge C. A., Leyser, O. 2009. Interactions between auxin and strigolactone in shoot branching control. Plant Physiol. 151, 400–412.

Hua D., Wang C., He J., Liao H., Duan Y., Zhu Z., Guo Y., Chen Z., Gong Z. 2012. A plasma membrane receptor kinase, GHR1, mediates abscisic acid and hydrogen peroxide regulated stomatal movement in Arabidopsis. Plant Cell 24: 2546-2561.

Huang W.E., Wang H., Zheng H., Huang L., Singer A.C., Thompson I., Whiteley A.S. Chromosomally located gene fusions constructed in Acinetobacter sp. ADP1 for the detection of salicylate. Environmental Microbiology. 2005;7: 1339–1348.

Huang W.E., Huang L., Preston G.M., Naylor M., Carr J.P., Li Y., Singer A.C., Whiteley A.S., Wang H. Quantitative in situ assay of salicylic acid in tobacco leaves using a genetically modified biosensor strain of Acinetobacter sp. ADP1. Plant J. 2006;46: 1073–1083.

Kohlen W., Charnikhova T., Liu Q., Bours R., Domagalska M.A., Beguerie S., Verstappen F., Leyser O., Bouwmeester H., Ruyter-Spira C. 2011. Strigolactones are transported through the xylem and play a key role in shoot architectural response to phosphate deficiency in nonarbuscular mycorrhizal host Arabidopsis. Plant Physiol. 155:974–87.

Kollist T., Moldau H., Rasulov B., Oja V., Rämma H., Hüve K., Jaspers P., Kangasjärvi J., Kollist H. 2007. A novel device detects a rapid ozone-induced transient stomatal closure in intact Arabidopsis and its absence in *abi2* mutant. Physiol Plant 129: 796–803.

Koornneef A., Pieterse C.M. 2008. Cross talk in defense signaling. Plant Physiol. 146(3):839-44.

Lechner E., Achard P., Vansiri A., Potuschak T., Genschik P. 2006. F-box proteins everywhere. Current Opinion in Plant Biology 9:631-638.

Li W., Nguyen K.H., Chu H.D., Ha C.V., Watanabe Y., Osakabe Y., Leyva-Gonzalez M.A., Sato M., Toyooka K., Voges L., Tanaka M., Mostofa M.G., Seki M., Seo M., Yamaguchi S., Nelson D.C., Tian C., Herrera-Estrella L., Tran L.S.P. 2017. The karrikin receptor KAI2 promotes drought resistance in Arabidopsis thaliana. PLoS Genet. 13(11):e1007076.

Lv S., Zhang Y., Li C., Liu Z., Yang, N., Pan, L., Wu, J., Wang, J., Yang, J., Lv, Y., Zhang, Y., Jiang, W., She, X., Wang, G. 2017. Strigolactone-triggered stomatal closure requires hydrogen peroxide synthesis and nitric oxide production in an abscisic acid-independent manner. New Phytol 217(1):290–304.

Mashiguchi K., Sasaki E., Shimada Y., Nagae M., Ueno K., Nakano T., Yoneyama K., Suzuki Y., Asami T. 2009. Feedback-regulation of strigolactone biosynthetic genes and strigolactone-regulated genes in Arabidopsis. Biosci Biotechnol Biochem 73: 2460–2465.

Melotto M., Underwood W., Koczan J., Nomura K., He, S. Y. 2006. Plant Stomata Function in Innate Immunity against Bacterial Invasion. Cell 126: 969-980.

Melotto M., Zhang L., Oblessuc P.R., He, S.Y. 2017.Stomatal Defense a Decade Later. Plant Physiol. 174: 561–571.

Merilo E., Laanemets K., Hu H., Xue S., Jakobson L., Tulva I., Gonzalez-Guzman M., Rodriguez P.L., Schroeder J.I., Brosche M., Kollist H. 2013. PYR/RCAR receptors contribute to ozone-, reduced air humidity-, darkness- and CO2-induced stomatal regulation. Plant Physiol. 162:1652–1668.

Merilo E., Jalakas P., Kollist H., Brosché, M. 2015. The role of ABA recycling and transporter proteins in rapid stomatal responses to reduced air humidity, elevated CO_2 and exogenous ABA. Mol. Plant. 8: 657–659.

Merilo E., Yarmolinsky D., Jalakas P., Parik H., Tulva I., Rasulov B., Kilk K., Kollist H. 2018. Stomatal VPD response: there is more to the story than ABA. Plant Physiol 176: 851–864.

Overmyer K., Tuominen H., Kettunen R., Betz C., Langebartels C., Sandermann H.Jr, Kangasjärvi J. 2000. Ozone-sensitive Arabidopsis *rcd1* mutant reveals opposite roles for ethylene and jasmonate signaling pathways in regulating superoxide-dependent cell death. Plant Cell. 12:1849–62.

Overmyer K., Kollist H., Tuominen H., Betz, C. Langebartels, C., Wingsle, G., Kangasjärvi, S., Brader, G., Mullineaux,P. and Kangasjärvi, J. 2008. Complex phenotypic profiles leading to ozone sensitivity in *Arabidopsis thaliana* mutants. *Plant, Cell and Environment* 31, 1237–1249.

Overmyer, K. L., Vuorinen, K. E., Brosche, M. J. 2018. Interaction points in plant stress signaling pathways. Physiologia Plantarum. 162, 2, p. 191–204.

Pieterse C.M, Leon-Reyes A., Van der Ent S., Van Wees S.C. 2009. Networking by small-molecule hormones in plant immunity. Nat Chem Biol. 5(5):308–16.

Pieterse C.M, Van der Does D., Zamioudis C., Leon-Reyes A., Van Wees S.C. 2012. Hormonal modulation of plant immunity. Annu. Rev. Cell Dev. Biol. 28:489–521.

Piisilä M., Keçeli M.A., Brader G., Jakobson L., Jõesaar I., Sipari N., Kollist H., Palva E.T. and Kariola T. 2015. The F-box protein MAX2 contributes to resistance to bacterial phytopathogens in *Arabidopsis thaliana*. BMC Plant Biology 15:53.

R Core Team. 2018. R: A language and environment for statistical computing. R Foundation for Statistical Computing, Vienna, Austria. URL https://www.R-project.org/.

Sierla M., Hõrak H., Overmyer K., Waszczak C., Yarmolinsky D., Maierhofer T., Vainonen J. P., Denessiouk K., Salojärvi J., Laanemets K., Tõldsepp K., Vahisalu T., Gauthier A., Puukko T., Paulin L., Auvinen P., Geiger D., Hedrich R., Kollist H., Kangasjärvi J. 2018. The receptor-like pseudokinase GHR1 is required for stomatal closure. The Plant Cell 30(11): 2813–2837.

Shen H., Luong P. and Huq E. 2007. The F-Box Protein MAX2 Functions as a Positive Regulator of Photomorphogenesis in Arabidopsis. Plant Physiol., 145; 1471–1483.

Sorefan K., Booker J., Haurogne K., Goussot M., Bainbridge K., Foo E., Chatfield S.P., Ward S., Beveridge C.A., Rameau C., Leyser O. 2003. MAX4 and RMS1 are orthologous dioxygenase-like genes that regulate shoot branching in Arabidopsis and pea. Genes Dev 17: 1469–1474.

Stes E., Depuydt S., De Keyser A., Matthys C., Audenaert K., Yoneyama, K. 2015. Strigolactones as an auxiliary hormonal defence mechanism against leafy gall syndrome in *Arabidopsis thaliana*. J. Exp. Bot. 66, 5123–5134.

Stirnberg P., van De Sande K., Leyser H.M. 2002. MAX1 and MAX2 control shoot lateral branching in Arabidopsis. Development (Cambridge, England) 129(5):1131-41.

Stirnberg P., Furner I.J., Leyser H.M.O. 2007. MAX2 participates in an SCF complex which acts locally at the node to suppress shoot branching. Plant J 50: 80–94.

Tan B.C., Joseph L.M., Deng W.T., Liu L.J., Li Q.B., Cline K., McCarty D.R. 2003. Molecular characterization of the Arabidopsis 9-cis epoxycarotenoid dioxygenase gene family. Plant J. 35:44–56.

Uknes S., Mauch-Mani B., Moyer M., Potter S., Williams S., Dincher S., Chandler D., Slusarenko A., Ward E., Ryals J. 1992. Acquired resistance in Arabidopsis. Plant Cell 4:645–56.

Umehara M., Hanada A., Yoshida S., Akiyama K., Arite T., Takeda-Kamiya N., Magome H., Kamiya Y., Shirasu K., Yoneyama K., Kyozuka J, Yamaguchi S. 2008. Inhibition of shoot branching by new terpenoid plant hormones. Nature 455: 195–200.

Vahisalu T., Puzõrjova I., Brosché M., Valk E., Lepiku M., Moldau H., Pechter P., Wang Y.S., Lindgren O., Salojärvi J., Loog M., Kangasjärvi J., Kollist H. 2010. Ozone-triggered rapid stomatal response involves the production of reactive oxygen species, and is controlled by SLAC1 and OST1. Plant J 62: 442–453.

Vainonen, J., Kangasjärvi, J. 2015. Plant signaling in acute ozone exposure. Plant, cell & environment. 38:240-252.

Waldie T., McCulloch H., Leyser O. 2014. Strigolactones and the control of plant development: lessons from shoot branching. Plant J. 79:607–22.

Wang Z.Y., Xiong L., Li W., Zhu J.K., Zhu J., 2011. The plant cuticle is required for osmotic stress regulation of abscisic acid biosynthesis and osmotic stress tolerance in Arabidopsis. Plant Cell 23: 1971–1984.

Wang L., Wang B., Jiang L., Liu X., Li X., Lu Z., Meng X., Wang Y., Smith S.M., Li J.4. 2015. Strigolactone signaling in arabidopsis regulates shoot development by targeting D53-Like SMXL repressor proteins for ubiquitination and degradation. Plant Cell 27(11):3128–3142.

Waters M. T., Nelson D. C., Scaffidi A., Flematti G. R., Sun Y. K., Dixon K. W., Smith S.M. 2012. Specialisation within the DWARF14 protein family confers distinct responses to karrikins and strigolactones in Arabidopsis. Development 139, 1285–1295.

Wickham H. 2016. ggplot2: Elegant Graphics for Data Analysis. Springer-Verlag New York.

Wildermuth M.C., Dewdney J., Wu G., Ausubel F.M. 2001. Isochorismate synthase is required to synthesize salicylic acid for plant defence. Nature 414:562–65.

Xie X., Yoneyama K., Kisugi T., Nomura T., Akiyama K., Asami T., Yoneyama K. 2015. Strigolactones are transported from roots to shoots, although not through the xylem. J Pestic Sci 40:214–216.

Xu E.J., Vaahtera L., Brosche M. 2015a. Roles of defense hormones in the regulation of ozone-Induced changes in gene expression and cell death. Mol. Plant, 8: 1776-1794.

Xu E., Vaahtera L., Horak H., Hincha D.K., Heyer A.G. and Brosche M. 2015b. Quantitative trait loci mapping and transcriptome analysis reveal candidate genes regulating the response to ozone in Arabidopsis thaliana. Plant, cell & environment 38 (7): 1418-1433.

Yeh Y.H., Chang Y.H., Huang P.Y., Huang J.B., Zimmerli L. 2015. Enhanced Arabidopsis pattern-triggered immunity by overexpression of cysteine-rich receptor-like kinases. Front. Plant Sci., 6, p. 322.

Yoshida R., Hobo T., Ichimura K., Mizoguchi T., Takahashi F., Aronso J., Ecker J.R., Shinozaki K. 2002. ABA-activated SnRK2 protein kinase is required for dehydration stress signaling in Arabidopsis. Plant Cell Physiol. 43(12):1473-83.

Zhang Y., Lv S., Wang G. 2018. Strigolactones are common regulators in induction of stomatal closure in planta. Plant Signal Behav. 13(3): e1444322.

Legends

Figure 1. Bacterial calculation after infection with *Pseudomonas syringae* DC3000. The infection was done by spraying followed by calculation of bacteria at 1.5 hours and 48 hours post inoculum. In each experiment four plants/line and three leaves/plant were used to measure the bacterial concentration. The experiment was repeated three times with similar results. The results are shown as means ± SE. In statistical analysis we conducted a logarithmic transformation on the data, then univariate analysis of variance combined to Hochberg post hoc test.

Figure 2. Accumulation of free salicylic acid in response to *Pseudomonas syringae* DC3000. Wild type (Col-0), strigolactone signaling mutants (*max2-1*, *max2-4*, *d14-1* and *d14-seto5*) and strigolactone biosynthesis mutants (*max3* and *max4*) were infected with *P. syringae* (OD600 = 0.2) by spraying. SA was measured using a biosensor-based method based on the protocol by DeFraia et al 2008. Salicylic acid biosynthesis mutant (*sid2-2*) was included as a control for no accumulation of free salicylic acid. Salicylic acid accumulation was measured 27 hours after infection. Each dot represents one plant. In total, seven to eight plants were used per line. The experiment were performed three times with similar results. Box plots are summarising data by showing the median, and first and third quartiles. Whiskers are extending to a maximum of 1.5 × interquartile range beyond the box. Different letters indicate significant differences ($P < 0.05$) as determined by Kruskal-Wallis Rank Sum test followed by Pairwise Wilcoxon Rank Sum tests with multiple testing correction to p-values using Holm method.

Figure 3. Relative gene expression in response to *Pseudomonas syringae* DC3000 spray infection and GR24 spray (dissolved in DMSO). (a) Relative expression (fold change GR24/control) after 3hr 10 µM GR24 treatment. The fold change is calculated from three biological repeats. (b) 4 week old plants were spray infected with *P. syringae* DC3000. Relative expression was calculated from three biological replicates for each plant line in each time point. In statistical analysis we conducted a logarithmic transformation on the data, then univariate analysis of variance combined to the Hochberg post hoc test.

Figure 4. Ozone sensitivity of strigolactone biosynthesis and perception mutants. Ion leakage was measured after ozone exposure (350 nL L^{-1} for 6 hours). In statistical analysis we conducted a logarithmic transformation on the data, then univariate analysis of variance combined to Hochberg post hoc test. The ion leakage in percentage is calculated by the ion leakage compared to the amount of total ions in the sample. The experiment was repeated three times and there were 4 biological repeats for each plant line in each time point.

Figure 5. Stomatal response to strigolactone analog (GR24) spray. (a) Time course of stomatal conductance of WT Col-0 plants. At time T=0 min the plants were sprayed with 10 µM GR24 or mock and returned back to the measuring cuvette (n=5). Data is presented as mean ± SEM. (b) The stomatal aperture width in response to GR24 stock dissolved in DMSO or acetone. The Col-0 plants were sprayed fully wet with 5 µM GR24 or an equivalent mock a day before the stomatal aperture measurements and the differently treated plants were kept covered separately with plastic overnight.

Figure 6. The stomatal conductance of strigolactone biosynthesis and perception mutants measured with a porometer from leaves of different developmental stages. The error bars represent standard error of the mean. 2-3 leaves per each growth stage was measured from each plant and altogether a minimum 20 plants were measured from each plant line. The phenotype based growth stage is determined in the article by Boyes et al 2001 in which numbers indicate the growth stage; 1 indicates leaf production, 3 rosette growth and 5 inflorescence emergence. We used the plants for analysis before they reached the stage 5.10 (i.e. before the first flower buds were visible). In statistical analysis we conducted a logarithmic transformation on the data, then univariate analysis of variance combined to Tukey HSD post hoc test.

Figure 7. Whole plant stomatal conductance and stomatal closure responses to darkness, high CO_2 and ABA foliar spray. (a) Stomatal conductance of *max2*, *max3* and *max4* mutants (n= 7-11). (b) Stomatal conductance of *max2* and *d14* mutants (n= 10-20). (c) Darkness-induced stomatal closure of *max2*, *max3* and *max4* mutants (10 min after induction; n = 7-11). (d) Darkness-induced stomatal closure of *max2* and *d14* mutants (10 min after induction; n = 10-20). (e) High CO_2-induced stomatal closure of *max2*, *max3* and *max4* mutants (10 min after induction; n = 6-12). (f) High CO_2-induced stomatal closure of *max2* and *d14* mutants (10 min after induction; n = 10-23). (g) ABA-induced stomatal closure of *max2*, *max3* and *max4* mutants (40 min after induction; n = 6-12). (h) ABA-induced stomatal closure of *max2* and *d14* mutants (40 min after induction; n = 13-23). All graphs present mean ± SEM. Asterisks denote statistically significant differences according to one-way ANOVA with Tukey HSD post hoc test. The time course data used to calculate the bar graphs (c)–(h) can be found in Supporting Information Figure 3.

Figure 8. The basal level of stomatal conductance of double mutants measured with intact plants. Four weeks old plants were measured, and the stomatal conductance is the average from 5-6 plants. Data is presented as mean ± SEM. In statistical analysis we conducted a logarithmic transformation on the data, then univariate analysis of variance combined to Tukey HSD post hoc test.

Figure 1

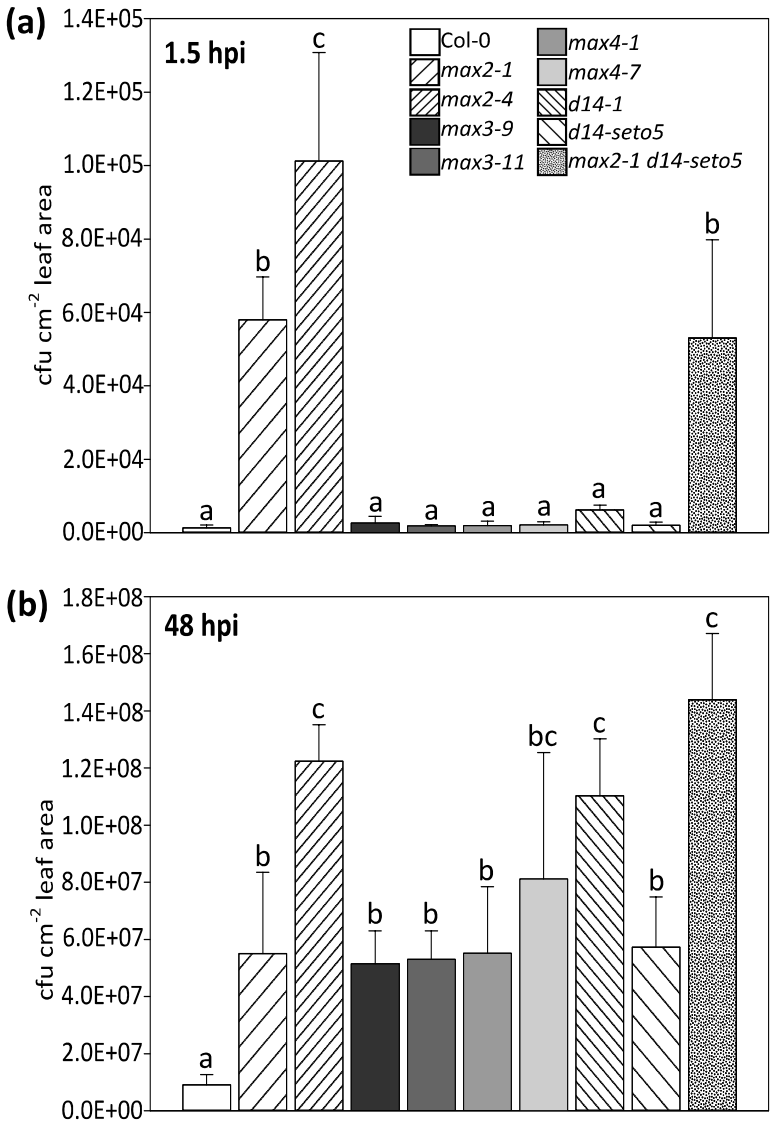
(a)
1.5 hpi
Col-0
max2-1
max2-4
max3-9
max3-11
max4-1
max4-7
d14-1
d14-seto5
max2-1 d14-seto5
cfu cm-2 leaf area
1.4E+05
1.2E+05
1.0E+05
8.0E+04
6.0E+04
4.0E+04
2.0E+04
0.0E+00
a
b
c
a
a
a
a
a
a
b
(b)
48 hpi
cfu cm-2 leaf area
1.8E+08
1.6E+08
1.4E+08
1.2E+08
1.0E+08
8.0E+07
6.0E+07
4.0E+07
2.0E+07
0.0E+00
a
b
c
b
b
b
bc
c
b
c

Figure 2

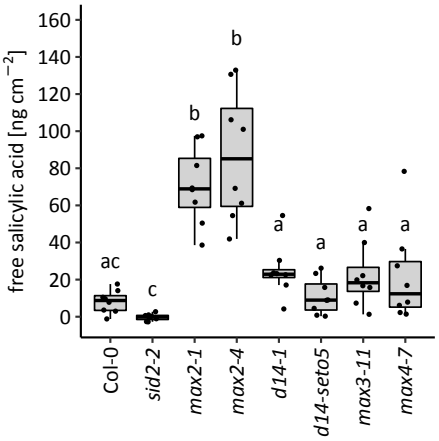
free salicylic acid [ng cm^{-2}]
160
140
120
100
80
60
40
20
0
ac
c
b
b
a
a
a
a
Col-0
sid2-2
max2-1
max2-4
d14-1
d14-seto5
max3-11
max4-7

Figure 3

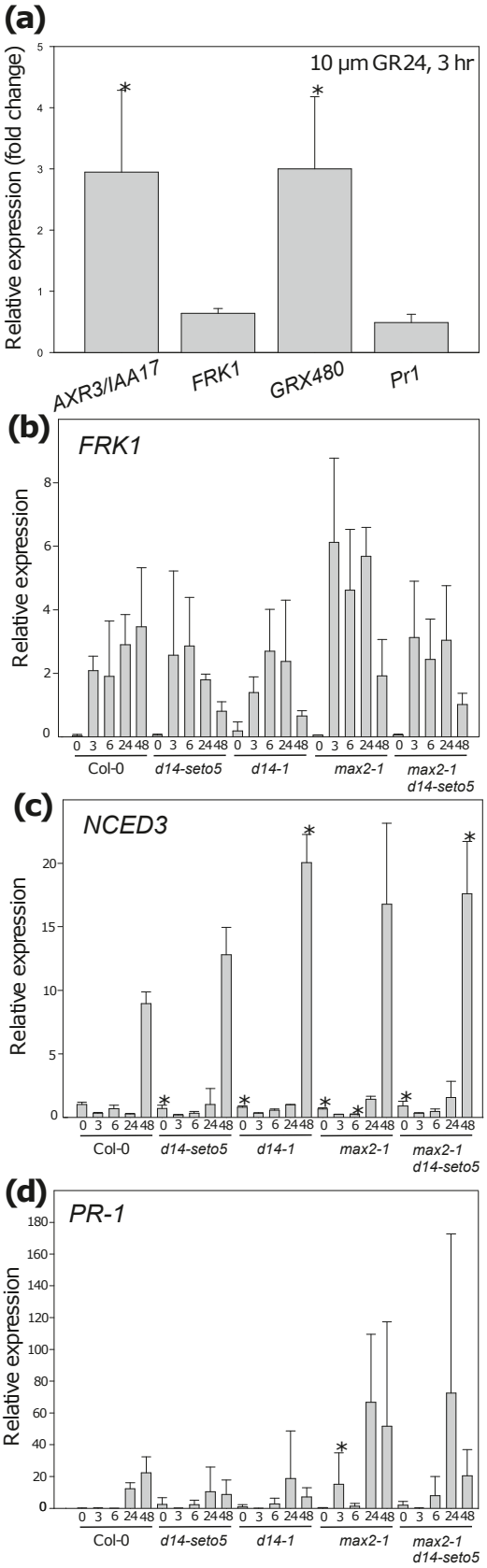
(a)
10 µm GR24, 3 hr
Relative expression (fold change)
AXR3/IAA17
FRK1
GRX480
Pr1
(b)
FRK1
Relative expression
0 3 6 24 48
Col-0
d14-seto5
d14-1
max2-1
max2-1 d14-seto5
(c)
NCED3
Relative expression
(d)
PR-1
Relative expression

Figure 4

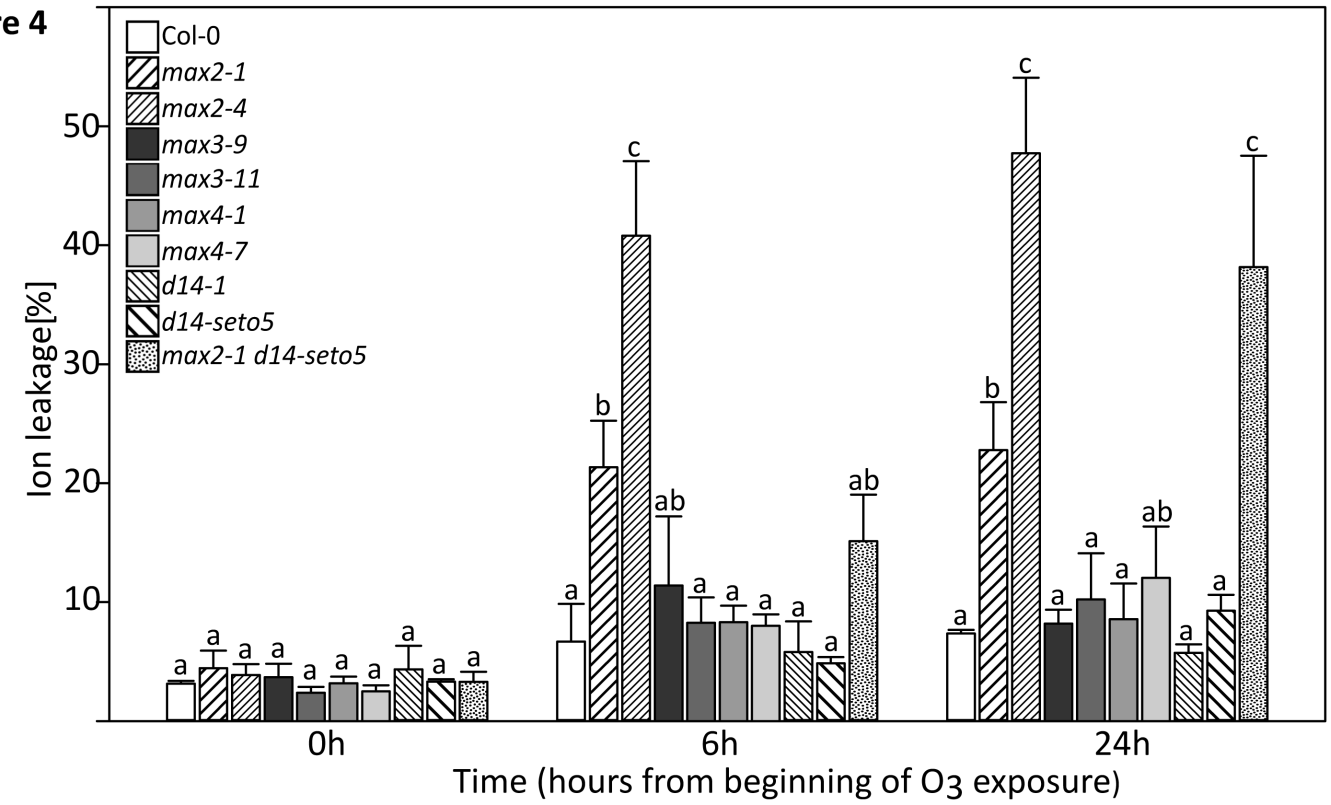
Col-0
max2-1
max2-4
max3-9
max3-11
max4-1
max4-7
d14-1
d14-seto5
max2-1 d14-seto5
Ion leakage[%]
50
40
30
20
10
0h
6h
24h
Time (hours from beginning of O3 exposure)

Figure 5

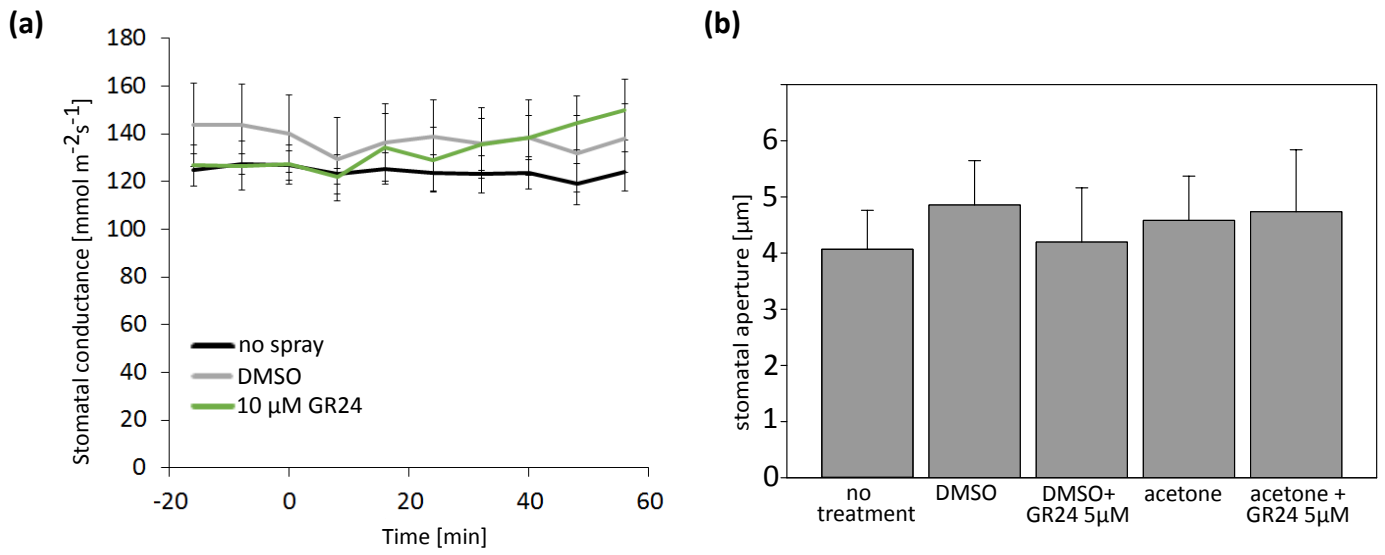
(a)
Stomatal conductance [mmol m-2s-1]
180
160
140
120
100
80
60
40
20
0
-20
0
20
40
60
Time [min]
no spray
DMSO
10 µM GR24
(b)
stomatal aperture [µm]
6
5
4
3
2
1
0
no treatment
DMSO
DMSO+ GR24 5µM
acetone
acetone + GR24 5µM

Figure 6

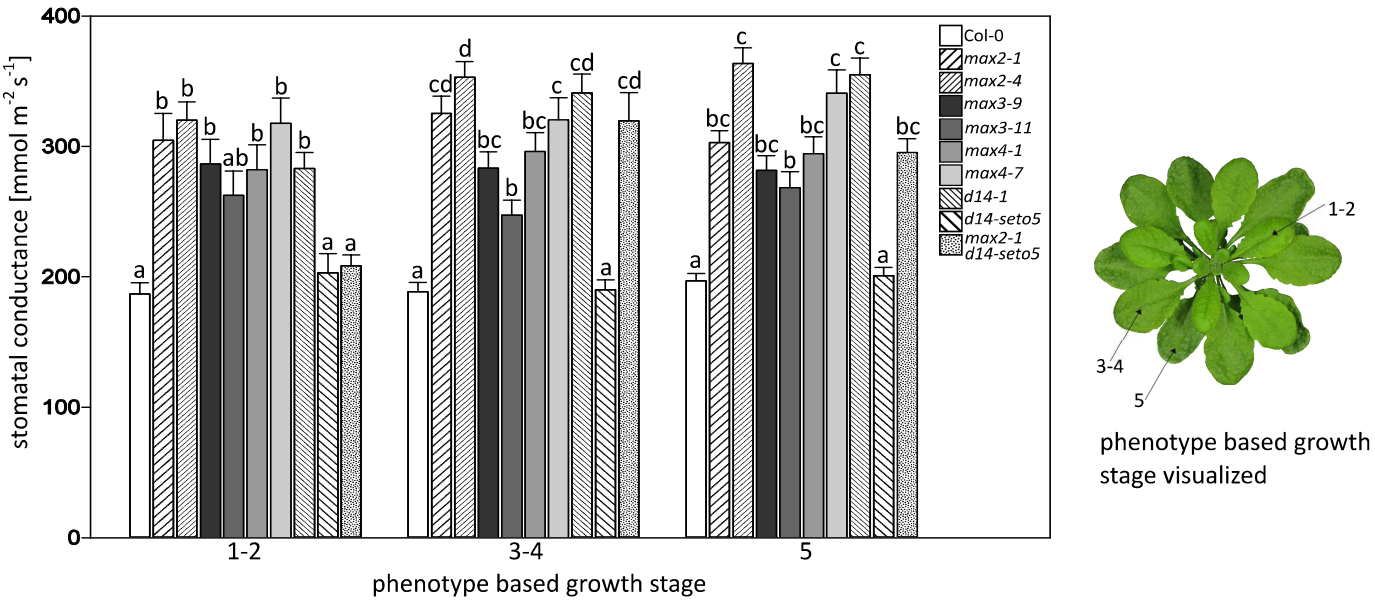
stomatal conductance [mmol m-2 s-1]
400
300
200
100
0
1-2
3-4
5
phenotype based growth stage
Col-0
max2-1
max2-4
max3-9
max3-11
max4-1
max4-7
d14-1
d14-seto5
max2-1 d14-seto5
1-2
3-4
5
phenotype based growth stage visualized

Figure 7

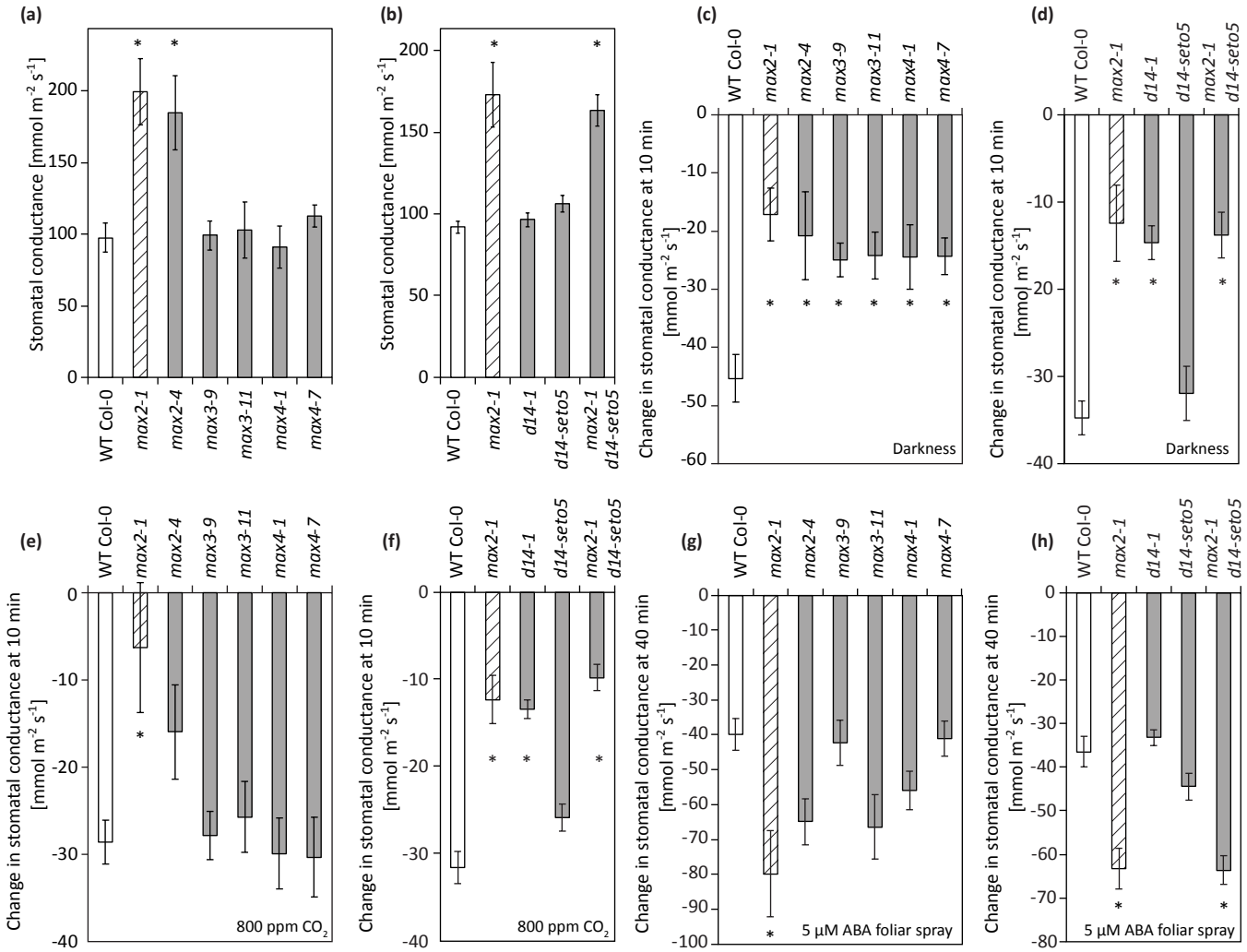
(a)
Stomatal conductance [mmol m-2 s-1]
WT Col-0
max2-1
max2-4
max3-9
max3-11
max4-1
max4-7
(b)
Stomatal conductance [mmol m-2 s-1]
WT Col-0
max2-1
d14-1
d14-seto5
max2-1 d14-seto5
(c)
Change in stomatal conductance at 10 min [mmol m-2 s-1]
Darkness
(d)
Change in stomatal conductance at 10 min [mmol m-2 s-1]
Darkness
(e)
Change in stomatal conductance at 10 min [mmol m-2 s-1]
800 ppm CO2
(f)
Change in stomatal conductance at 10 min [mmol m-2 s-1]
800 ppm CO2
(g)
Change in stomatal conductance at 40 min [mmol m-2 s-1]
5 µM ABA foliar spray
(h)
Change in stomatal conductance at 40 min [mmol m-2 s-1]
5 µM ABA foliar spray

Figure 8

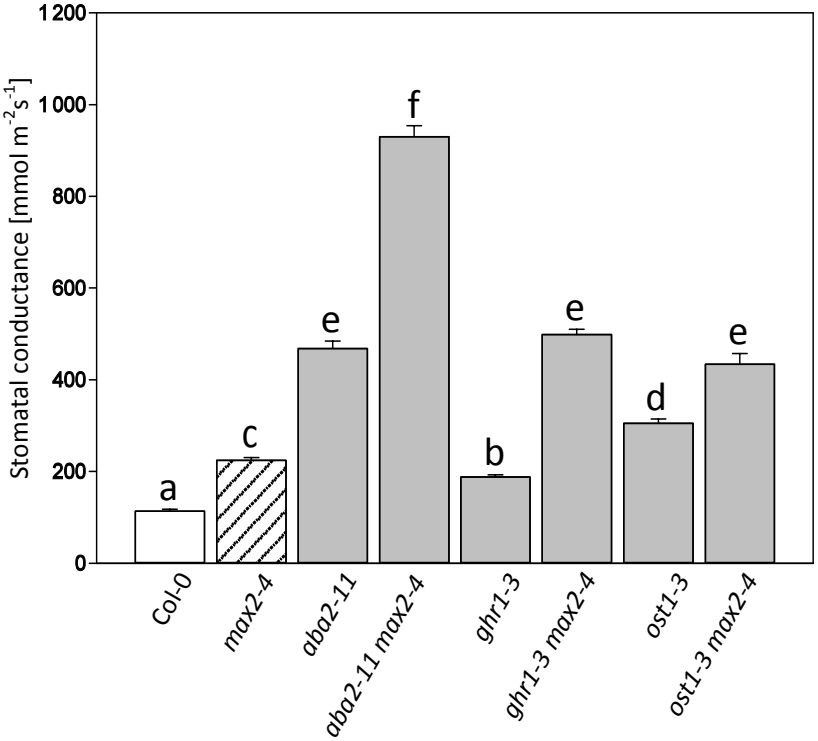
Stomatal conductance [mmol m-2s-1]
1200
1000
800
600
400
200
0
a
c
e
f
b
e
d
e
Col-0
max2-4
aba2-11
aba2-11 max2-4
ghr1-3
ghr1-3 max2-4
ost1-3
ost1-3 max2-4

Supporting Information Figure 1

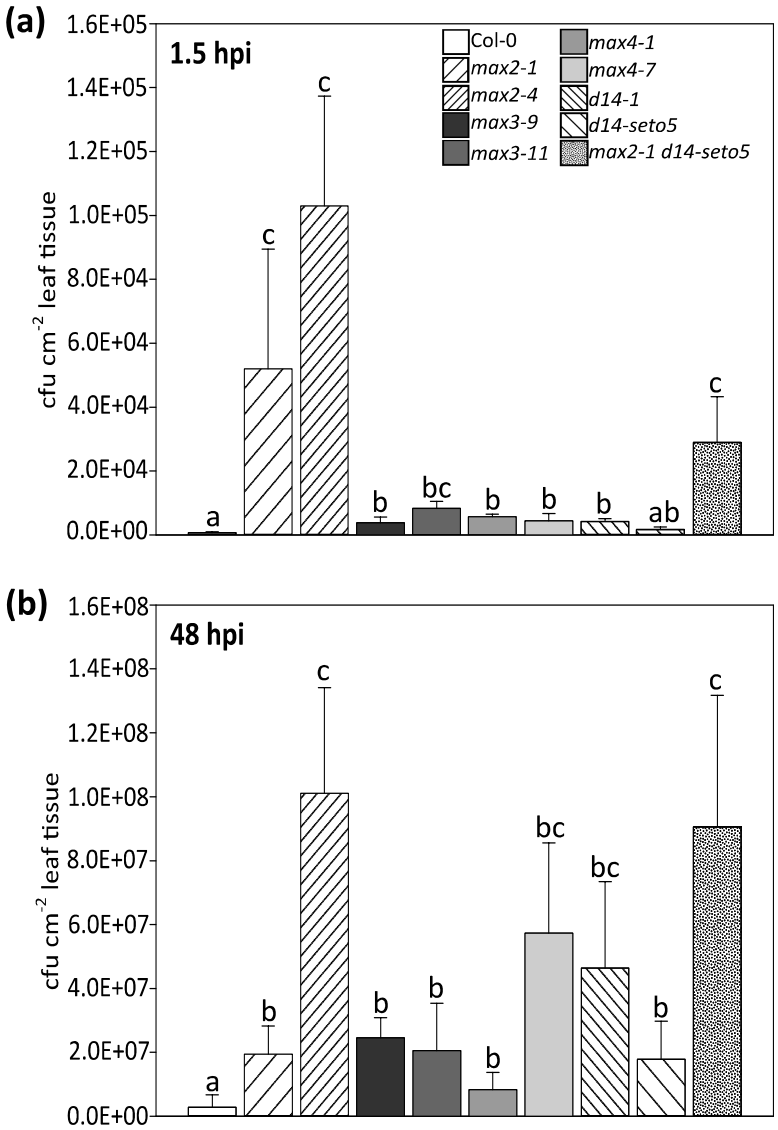

Supporting Information Figure 2

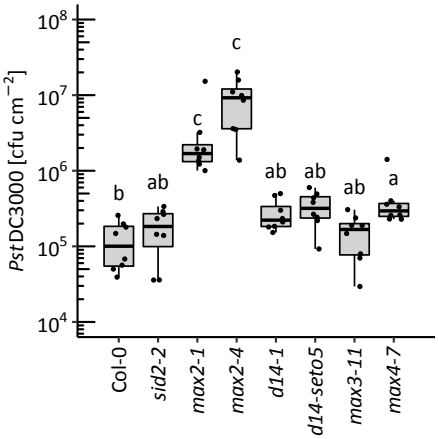

Supporting Information Figure 3

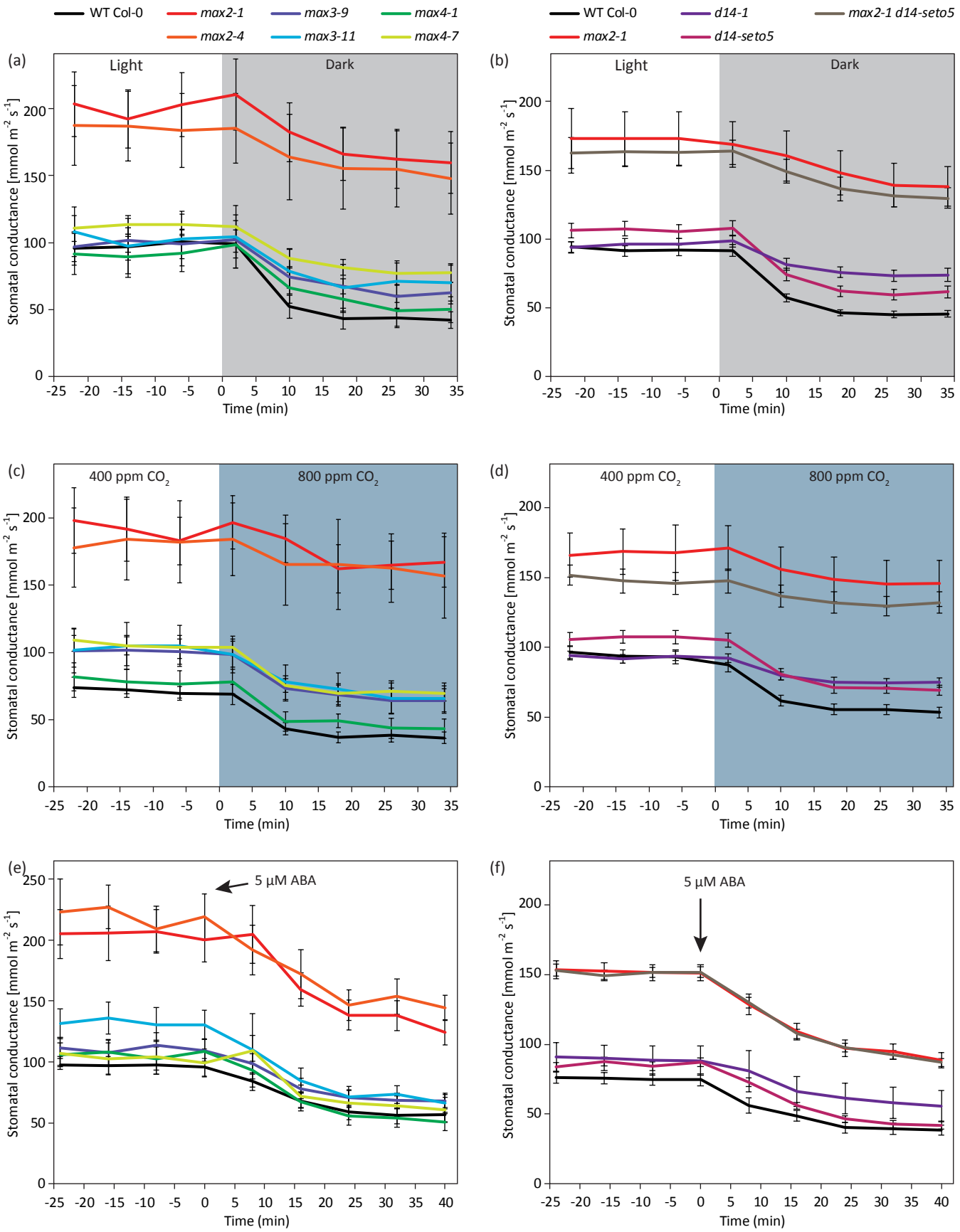

Supporting Information Figure 4

Supplemental Table 1. Primers used in this study

Primer name	Primer Sequence (5' → 3')	Comments
Genotyping of mutant lines		
D14-seto5 F	TATGATCGGAATCATCGCTTC	
D14-seto5 R	GACCTAAGATACTCCGCCACC	
D14-1 MW221	AAGAATATGGCAAGTGCAAC	Genomic primer for Atd14-1 allele, Waters et al 2012
D14-1 MW222	GATGATTCCGATCATAGCG	Genomic primer for Atd14-1 allele, Waters et al 2012
L4_WiscLoxHS	TGATCCATGTAGATTTCCCGGACATGAAG	T-DNA primer for Atd14-1 allele, Waters et al 2012
max2-1 F	GTTGGAGAATTTTTGACGCCAT	
max2-1 R	CAAAGGCCGAGCTGTAAAGAGA	
max2-4 F	TACCTCCTGTGCTTCTCCGCTA	SALK_028336
max2-4 R	CTTCTGGCTCCTCTCGTAACCA	SALK_028336
max3-9 F	CCCTTCCGGTACATACTACTT	
max3-9 R	GTAGTGAGTATCCGTGAATGC	
max3-11 F	CGTTAAACCCAAGCAACGAGAG	
max3-11 R	CATCGGAAACGTCAAATTCCTC	
max4-1 F	AAGGAAAGATACCCACTTGGC	
max4-1 R	GTACCAACCATGCCTATGACC	
SPM8225F	TCGGCTTATTTCAGTAAGAGTG	SPM8225F transposon insertion primer for max4-1, Sorefan et al 2003
max4-7 F	ACTGGTCATAGGCATGGTTGGT	SALK_082552
max4-7 R	ACCGAATATCTCAGGGGCATTT	SALK_082552
aba2-11_F	TTGATGTGACAGGCTTTTGG	
aba2-11_R	TCTTGCAGATCAACAATGCAG	
ghr1-3_F	TGGCCCTTCTAAGCTGTTAGA	
ghr1-3_R	CTCCTTATCTGGACCTTTGCC	
ost1-3_F	CATATCTTTAGACGAGGGGCC	
ost1-3_R	GTGAGTGGTCCAATGGATTTG	
SALK_LBb1.3	ATTTTGCCGATTTCGGAAC	
GK_o8474	ATAATAACGCTGCGGACATCTACATTTT	
qPCR primers		
YLS8 for	TTACTGTTTCGGTTGTTCTCCATTT	efficiency 1.822
YLS8 rev	CACTGAATCATGTTCGAAGCAAGT	
PP2AA3 for	GCGGTTGTGGAGAACATGATACG	efficiency 1.854
PP2AA3 rev	GAACCAAACACAATTCGTTGCTG	
TIP41 for	GTGAAAACTGTTGGAGAGAAGCAA	efficiency 1.867
TIP41 rev	TCAACTGGATACCCTTTCGCA	
AXR3-F	CACATTGATTGGTGTTAATTGC	efficiency 1.744
AXR3-R	CCAAATCCAGATCAAAACACAG	
GRX480 for	ACGGAGAGGATGTTGCATGTGTC	efficiency 1.843
GRX480 rev	AATCTCAAGGACCGCCGGATTC	
PR-1 for	CGGAGCTACGCAGAACAACT	efficiency 1.658
PR-1 rev	CTCGCTAACCCACATGTTCA	
NCED3 for	AGCTCCTTACCTATGGCCAGT	efficiency 1.968
NCED3 rev	CGCTCTCTGGAACAAATTCATC	
FRK1 for1	CGGTCAGATTTCAACAGTTGTC	efficiency 1.843, used in GR24 assay (Figure 3a)
FRK1 rev1	AATAGCAGGTTGGCCTGTAATC	
FRK1 for2	GCCAACGGAGACATTAGAG	efficiency 1.876, used in P.syringae infection experiment (Figure 3b), primer sequences
FRK1 rev2	CCATAACGACCTGACTCATC	published by Yeh et al., (2015)

References

Yeh Y.H., Chang Y.H., Huang P.Y., Huang J.B., Zimmerli L. 2015. Enhanced Arabidopsis pattern-triggered immunity by overexpression of cysteine-rich receptor-like kinases. Front. Plant Sci., 6:322.